

Toppling Manipulation

Kevin M. Lynch
 Laboratory for Intelligent Mechanical Systems
 Department of Mechanical Engineering
 Northwestern University
 Evanston, IL 60208-3111

Abstract

This paper describes a robotic manipulation primitive called *toppling*—knocking a part over. We derive the mechanical conditions for toppling, express these as constraints on robot contact locations and motions, and describe an application of toppling to minimalist parts feeding of 3D objects on a conveyor with a 2 joint robot.

1 Introduction

In the spirit of minimalist robotics, we are studying a manipulation primitive called *toppling*. Toppling occurs when a robot knocks a part over to a new face. This work has two motivations: (1) it adds to the repertoire of manipulation primitives (which includes grasping, pushing, throwing, tapping, and tumbling; see Lynch and Mason [9] for an overview) available to a robot in manipulation planning; and (2) it can be accomplished using very simple, low-degree-of-freedom robot motions. One natural application for toppling is reorienting parts on conveyors. Since the conveyor provides linear motion for the part, the toppling “robot” can in fact be a fixed overhang (for example, the overhangs above a bowl feeder track). Thus robot motion is reduced to fixed automation. When combined with previous work on orienting planar parts on conveyors (Akella *et al.* [3]; Peshkin and Sanderson [14]; Brokowski *et al.* [6]; Wiegley *et al.* [20]), toppling permits full 3D parts feeding on a conveyor.

In this paper we study the mechanics of toppling and derive an algorithm for finding the set of contact points on a part from which it can be toppled to a new face. The results of this algorithm provide the basis for automatic motion planning to find a sequence of topples to a desired goal face, or for finding a sequence of fixed overhangs. Based on our results, we have constructed the 2JOC, a two joint robot which can position and orient 3D parts on a moving conveyor (Figure 1).

This work is inspired by K. Goldberg’s [8] suggestion of the utility of toppling in minimalist manipulation and parts feeding. Our mechanics analysis is related to Erdmann’s [7] work on two-palm nonprehensile manipulation. Erdmann constructed a planner to find motions for two independent three degree-of-freedom planar palms manipulating an object without grasping it. The planner uses a quasistatic model of frictional mechanics and finds motions that utilize a variety of slipping and rolling motions between the object and the palms. In our work we consider a much simpler set

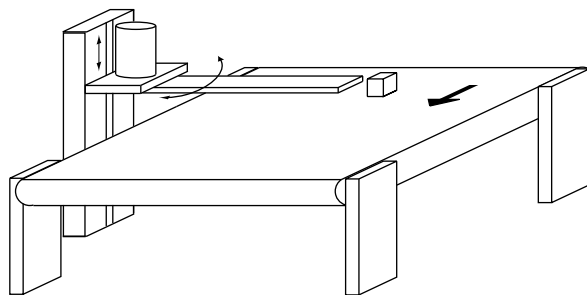


Figure 1: The 2JOC feeds parts on a conveyor by pushing and toppling.

of robot motions and focus on the conditions for inducing toppling of an object on a moving conveyor.

Other related work includes pivoting and tumbling parts using a robot hand (Brock [5]; Sawasaki *et al.* [16]; Aiyama *et al.* [2]; Trinkle [18, 19]). By grasping a part with a pivoting gripper that allows the part to reorient under gravity, Rao *et al.* [15] showed that a 4 DOF SCARA robot could induce out-of-plane rotations. Zhang and Gupta [21] recently presented an approach to orienting parts on a conveyor by allowing them to fall over steps. Toppling can also be effected by controlled acceleration of the conveyor. A similar idea for toppling parts was presented by Singer and Seering [17].

Our 2JOC robot controls the position and orientation of parts on a conveyor by pushing and toppling. The motivations are closely related to those of Bicchi and Sorrentino [4] who demonstrated control of the position and orientation of an object by rolling it between two grasping palms. Because spatial rolling constraints are nonholonomic, the three degree-of-freedom robot is able to control the object’s position and orientation. With the 2JOC, the conveyor-plane position and orientation of a polyhedral part is controlled by pushing the part over the conveyor, while Marigo *et al.* [10] have studied the set of reachable configurations for polyhedra on a planar surface when the parts can only roll about edges.

In Section 2 we derive the contact conditions for toppling and the toppling transition directed graph, which indicates the new resting face once the part has toppled. In Section 3 we describe some applications of toppling to parts feeding, including the 2JOC. We conclude in Section 4.

2 Toppling

Toppling consists of two phases: rolling (Section 2.1) and settling (Section 2.2). During rolling the robot pushes the part up onto a *toppling edge*, which is perpendicular to the motion of the conveyor, until the center of mass of the part is directly above the edge. During settling the part falls under gravity, lands on a new face, and perhaps continues to roll onto another face before coming to rest.

We define two planes: the *toppling plane* and the *conveyor plane*. The toppling plane is a plane orthogonal to the toppling edge. In our analysis of toppling we project the part onto this plane, and the toppling edge projects to a toppling, or pivot, vertex. We assume the projection of the part to the toppling plane is polygonal. The conveyor plane is the plane of the conveyor, and it is orthogonal to the toppling plane. All toppling analysis occurs in the toppling plane; the conveyor plane is relevant when we include pushing motions in this plane with the 2JOC.

2.1 Rolling Conditions

The part rests on a horizontal conveyor moving to the right on the page (Figure 2). We define a frame fixed to the conveyor with origin at the pivot vertex of the part (which moves with the conveyor) with the x -axis aligned with the direction of motion of the conveyor and the y -axis vertical. The center of mass of the part in this frame is at a distance r from the origin at an angle η . The friction coefficients μ_c and μ_f correspond to friction between the part and the conveyor and between the part and the fence, respectively. The corresponding friction cone half-angles are $\alpha_c = \tan^{-1} \mu_c$ and $\alpha_f = \tan^{-1} \mu_f$.

The fence contacts a part edge with one endpoint at (x, y) in the conveyor frame. The angle of the edge is ψ from (x, y) and the inward-pointing contact normal for the edge is at $\psi + \pi/2$. The friction cone between the part and the fence is bounded by the angles of the left friction cone edge $\beta_l = \psi + \pi/2 + \alpha_f$ and the right friction cone edge $\beta_r = \psi + \pi/2 - \alpha_f$.

The question is, what fence contact points along this edge will result in the part initially rolling over the pivot vertex?

The key construction is shown in Figure 2. Draw a vertical line through the center of mass, extend the right edge of the friction cone at the pivot until it intersects this line, and extend the left edge of the friction cone backward until it intersects this line. This defines a triangle with vertices P_1 at $(r \cos \eta, (r \cos \eta) / \mu_c)$, P_2 at $(0, 0)$ (the pivot), and P_3 at $(r \cos \eta, (-r \cos \eta) / \mu_c)$ in the conveyor frame. If the fence is rigid, and the contact force the fence applies to the part makes positive moment about every point in this triangle (i.e., the contact force passes around the triangle in a counterclockwise fashion), then the only quasistatic solution is that the part rolls about the pivot vertex.¹ To guarantee rolling, every force in the fence friction cone must make positive moment about every point in the $P_1 P_2 P_3$ triangle. In Figure 2, the fence friction cone shown barely satisfies this condition.

¹We state this without proof. See (Mason [11]) for related examples.

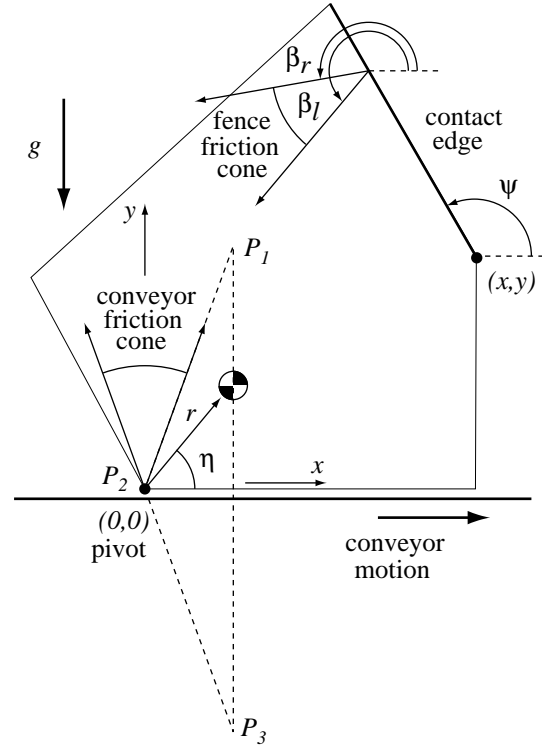


Figure 2: Notation for rolling.

The contact friction cone in Figure 2 marginally satisfies the rolling condition, and it is apparent that any higher contact point will also satisfy the condition. We can state this formally. Parameterize the contact edge by w , so that points on the contact edge are given by $(x, y) + w(\cos \psi, \sin \psi)$, $w \in [0, w_{max}]$. Then if a contact force (any force with a positive component in the direction of the inward-pointing contact normal) through $(x, y) + w_0(\cos \psi, \sin \psi)$ makes positive moment about a point P , it is easy to show that any other parallel force through $(x, y) + w(\cos \psi, \sin \psi)$, $w > w_0$, also makes positive moment about P . Therefore, if contact at w_0 causes rolling, then contact at $w > w_0$ also causes rolling. Thus the construction of Figure 2 confirms these intuitive properties of rolling:

- “higher” fence contacts tend to produce rolling, while lower contacts result in slipping on the conveyor;
- a larger conveyor friction coefficient μ_c results in a smaller $P_1 P_2 P_3$ triangle, increasing the set of contact points that produce rolling;
- a center of mass further to the left results in a smaller $P_1 P_2 P_3$ triangle, increasing the set of contact points that produce rolling.

The construction also shows that the height of the center of mass plays no role in the quasistatic, dry friction rolling conditions.

The analysis of Figure 2 only addresses the instantaneous initial condition for rolling. As the part rolls, it may become wedged or begin slipping on the conveyor. To analyze

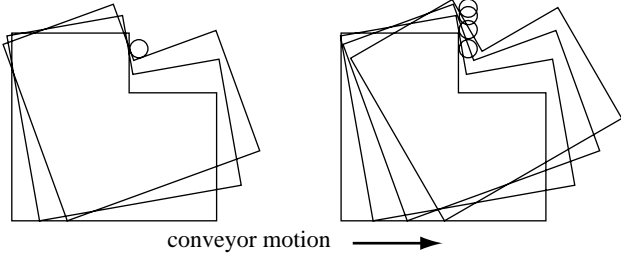


Figure 3: The part on the left becomes wedged or begins slipping with a fence of fixed height. The fence on the right lifts up to maintain a constant contact point on the part, allowing it to topple over.

the gross motion of the part after it begins rolling, we consider two models of the motion of the fence. In the first model, the fence “complies” to the shape of the part in a position-controlled manner, so that the contact point on the part remains constant during rolling. In the second model, the fence remains motionless. The first model is easier to analyze, and it increases the set of parts that can be toppled. The second model requires no motion by the fence.

2.1.1 Position-Controlled Fence

To simplify analysis and to be able to topple parts that might otherwise slip or become wedged, we raise or lower the fence so *the contact point on the part remains constant* as the part rolls. The velocity of the conveyor is known, and given the geometry and initial position of the part, the fence can simply “comply” to the shape of the part in a position-controlled manner. The fence maintains contact until the angle η to the center of mass becomes greater than $\pi/2$. The part then falls to a new stable edge. See Figure 3.²

The goal is to find contact points that maintain the rolling condition as the center of mass rolls from its initial angle η_i to its final angle $\eta_f = \pi/2$, at which point the part topples over. As the part rolls, the fence friction cone moves in the conveyor frame. (The $P_1P_2P_3$ triangle also shrinks.) As a result, a contact that causes rolling at η_i may not cause rolling as η increases—the part may begin to slide or wedge. So, for a given pivot vertex and contact edge, we must find w_0 such that all contact points $w > w_0$ result in rolling at all angles $\eta \in [\eta_i, \eta_f]$.

Consider the top triangle vertex P_1 , at $(r \cos \eta, (r \cos \eta)/\mu_c)$. At $\eta = \eta_i$ the contact edge is at an angle ψ from the vertex at (x, y) . Consider the right edge of the fence contact friction cone, at an angle β_r . We would like to find the function $w_{1r}(\eta)$ which gives the edge contact point where the right edge of the friction cone passes exactly through P_1 . We define w_{1r}^* to be the maximum value of $w_{1r}(\eta)$ for $\eta \in [\eta_i, \eta_f]$. Then the positive moment rolling condition for the triangle vertex P_1 and the right edge of the friction cone is satisfied for all contact points $w > w_{1r}^*$. (Similarly we can define w_{1l}^* for vertex P_1 and the left edge

²If the next clockwise edge contacts the conveyor before η reaches $\pi/2$, that edge is unstable. In this case the next vertex clockwise on the part’s convex hull becomes the pivot vertex. For simplicity, we will ignore this case.

of the friction cone; for vertex P_2 we have w_{2r}^*, w_{2l}^* , and for vertex P_3 we have w_{3r}^*, w_{3l}^* .)

The line of the contact edge during rolling can be expressed as a function of the angle η and the contact parameter w :

$$\begin{aligned} &(x \cos \Delta\eta - y \sin \Delta\eta + w \cos(\psi + \Delta\eta), \\ &x \sin \Delta\eta + y \cos \Delta\eta + w \sin(\psi + \Delta\eta)), \end{aligned} \quad (1)$$

where $\Delta\eta = \eta - \eta_i$ is the amount of rolling the part has undergone. The contact force is at an angle $\beta_r + \Delta\eta$, and the line of action of the force through the triangle vertex P_1 can be parameterized by v :

$$(r \cos \eta + v \cos(\beta_r + \Delta\eta), (r \cos \eta)/\mu_c + v \sin(\beta_r + \Delta\eta)). \quad (2)$$

We solve for the contact point that provides a force through P_1 by equating (1) and (2) and solving for w :

$$\begin{aligned} w_{1r}(\eta) = &(2\mu_c y \cos \beta_r - r \cos \lambda - r \cos v - 2\mu_c x \sin \beta_r \\ &+ \mu_c r \sin \lambda + \mu_c r \sin v) / 2\mu_c \sin(\beta_r - \psi), \end{aligned} \quad (3)$$

where $\lambda = \beta_r - \eta_i$ and $v = \beta_r + 2\eta - \eta_i$. A necessary condition for $w_{1r}(\eta)$ to reach its maximum is $dw_{1r}(\eta)/d\eta = 0$:

$$\frac{dw_{1r}(\eta)}{d\eta} = \frac{2\mu_c r \cos v + 2r \sin v}{2\mu_c \sin(\beta_r - \psi)} = 0. \quad (4)$$

Solving (4) for η , we get $\eta_{1r} = (\tan^{-1}(-\mu_c) - \beta_r + \eta_i)/2$. Then w_{1r}^* must occur at either η_i , η_f , or η_{1r} . To find w_{1r}^* , we need only evaluate (3) at a discrete set of angles.

Similarly for the bottom triangle vertex P_3 , we get

$$\begin{aligned} w_{3r}(\eta) = &(2\mu_c y \cos \beta_r + r \cos \lambda + r \cos v - 2\mu_c x \sin \beta_r \\ &+ \mu_c r \sin \lambda + \mu_c r \sin v) / 2\mu_c \sin(\beta_r - \psi), \end{aligned} \quad (5)$$

$$\frac{dw_{3r}(\eta)}{d\eta} = \frac{2\mu_c r \cos v - 2r \sin v}{2\mu_c \sin(\beta_r - \psi)} = 0, \quad (6)$$

and $\eta_{3r} = (\tan^{-1}(\mu_c) - \beta_r + \eta_i)/2$. For the triangle vertex P_2 (the pivot point):

$$w_{2r} = \frac{y \cos \beta_r - x \sin \beta_r}{\sin(\beta_r - \psi)}, \quad (7)$$

and w_{2r} (hence w_{2r}^*) is independent of η .

Substituting β_l for β_r in the equations above, we find $w_{1l}^*, w_{2l}^*, w_{3l}^*$. Define w_{max}^* to be the maximum of the six values $w_{\{1,2,3\}\{r,l\}}^*$. If w_{max}^* is greater than w_{max} defining the end of the edge segment, then there are no toppling contacts on this edge. Otherwise, the range of toppling contacts is given by the range $(\max(0, w_{max}^*), w_{max})$.

We have implemented an algorithm in Lisp which, for each stable resting configuration of the polygon, finds the toppling contacts on each edge. An example is shown in Figure 5. As expected, increasing conveyor friction increases the range of toppling contacts.

This analysis ensures that any force inside the fence friction cone causes rolling, and is therefore conservative. Instead, we could simply verify that, at all times, there exists

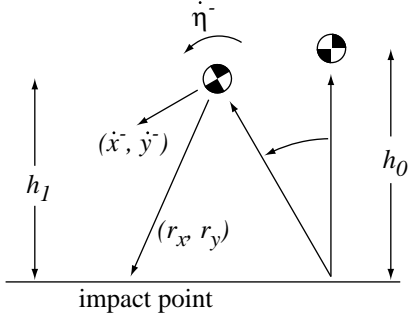


Figure 4: Notation for settling analysis.

a contact force inside the fence friction cone that produces rolling. The fence could move such that it barely slips on the part as it moves; the contact point is not quite maintained. This allows the fence to choose a force at the edge of its friction cone. Therefore, the rolling analysis does not have to be satisfied for all possible forces in the friction cone, but just for the chosen edge of the friction cone.

2.1.2 Fixed Fence

If the fence remains a fixed height as the part moves on the conveyor, we must find a range of fence heights y that guarantees toppling. To do that we again equate (1) and (2) for a particular contact edge, but now solve for $y(\eta)$ instead of $w(\eta)$. There is no closed-form solution to $dy(\eta)/d\eta = 0$, however, so the minimum y value that ensures toppling must be determined numerically.

The following conditions must also be satisfied: the fence cannot lose contact with the part as it rolls, and rolling must continue if the fence switches contact to a new edge during rolling (the part cannot wedge in a concavity or begin to slip).

2.2 Settling

When the center of mass passes the vertical with respect to the pivot point, the part begins to free fall. The part may simply come to rest on the next edge, or it may continue past this edge and come to rest on a subsequent edge.

The part falls like a pendulum, as shown in Figure 4, until impacting at the next vertex clockwise of the pivot vertex on the part's convex hull. The pre-impact linear velocity of the part's center of mass is (\dot{x}^-, \dot{y}^-) , and the angular velocity is $\dot{\eta}^-$, given by

$$\dot{\eta}^- = \sqrt{\frac{2mg(h_0 - h_1)}{I_p}},$$

where m is the mass of the part, g is the gravitational constant, and h_0 and h_1 are the height of the center of mass above the conveyor at the beginning and end of the free fall, respectively. I_p is the inertia of the part about the pivot, where $I_p = m(\rho^2 + h_0^2)$, and ρ is the radius of gyration of inertia of the part measured about its center of mass. The vector from the center of mass to the impact vertex is (r_x, r_y) .

To determine the settling edge, we assume a perfectly plastic impact between the impact vertex and the conveyor.

This places three constraints on the post-impact velocity. The first two are kinematic, and the third indicates that the impulse passes through the impact point:

$$\begin{aligned} \dot{x}^+ &= r_y \dot{\eta}^+ \\ \dot{y}^+ &= -r_x \dot{\eta}^+ \\ r_x(\dot{y}^+ - \dot{y}^-) - r_y(\dot{x}^+ - \dot{x}^-) &= \rho^2(\dot{\eta}^+ - \dot{\eta}^-). \end{aligned}$$

Solving yields

$$\dot{\eta}^+ = \frac{\rho^2 \dot{\eta}^- + r_y \dot{x}^- - r_x \dot{y}^-}{\rho^2 + r_x^2 + r_y^2}.$$

The pendulum now begins a new free fall stage about the new impact vertex with this initial angular velocity. The part has settled when the post-impact velocity causes immediate re-impact with the previous vertex on successive impacts.

2.3 Toppling Transition Directed Graph

With the rolling conditions and the settling analysis, we can construct the *toppling transition directed graph* for a planar part. Each node of the graph corresponds to a stable resting edge for the part. From each node there is a single arc that leads to the node the part reaches after toppling. This arc is tagged with the contact points on the part (in the case of a position-controlled fence) or the fence heights (in the case of fixed fences) that result in toppling. If no fence contacts can result in toppling from this node, the arc is eliminated. Increasing conveyor friction μ_c can result in the addition of arcs to the graph. Figure 5 shows an example for a position-controlled fence.

Finding a fence plan amounts to searching this graph for a sequence of actions leading from the start node to the goal node.

3 Applications

3.1 Sensorless Parts Feeding

A sequence of stationary fences over a conveyor can be used to reduce uncertainty in the orientation of a part in the toppling plane. This is similar to the work of Zhang and Gupta [21], who showed that uncertainty in the orientation of a part can be reduced by having the part fall over a series of steps on the conveyor. These sensorless strategies for reducing uncertainty in the toppling plane can be combined with sensorless approaches to conveyor-plane parts feeding (Akella *et al.* [3]; Peshkin and Sanderson [14]; Brokowski *et al.* [6]; Wiegley *et al.* [20]) to construct sensorless 3D parts feeding devices on conveyors.

An example sequence of fixed fences is shown in Figure 6. The part is a 3-4-5 triangle, with edges labeled as shown in Figure 6 and vertices at $(-2, -0.5)$, $(1, -0.5)$, and $(1, 3.5)$ with respect to an origin at the center of mass. The friction coefficients are $\mu_f = 0$ and $\mu_c = \tan 30^\circ = 0.577$. A fixed-height peg at a height y above the conveyor, $3.467 < y < 3.881$, causes a triangle at rest on edge 1 to topple to rest on edge 3, while a triangle at rest on edges 2 or 3 passes under the peg. (If $y > 4$, the triangle passes under the peg; if

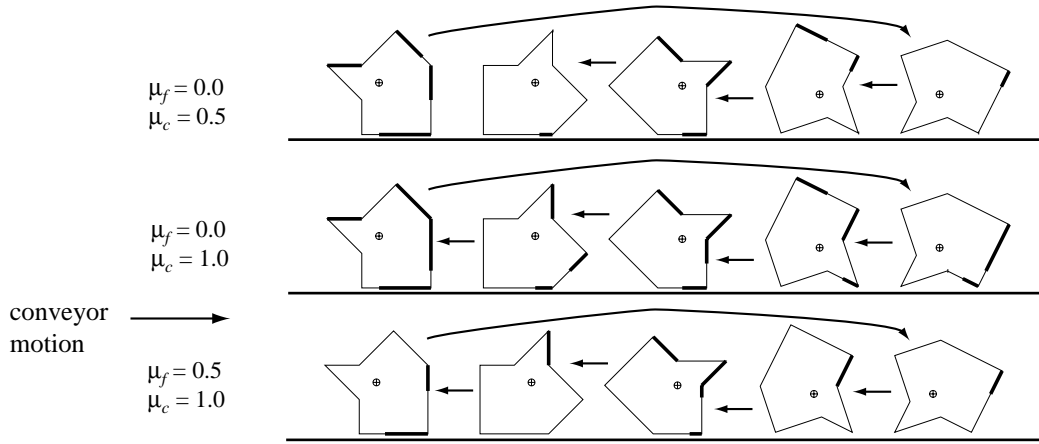


Figure 5: Toppling contacts for a position-controlled fence and two different conveyor friction coefficients μ_c . The toppling contacts are indicated by heavy lines. As we increase μ_c , the ranges of toppling contacts increase. The arrows indicate a toppling transition directed graph. In the case $\mu_c = 0.5$, there is a single resting configuration from which the part cannot be toppled. The fence would have to contact the bottom edge of the part to cause toppling.

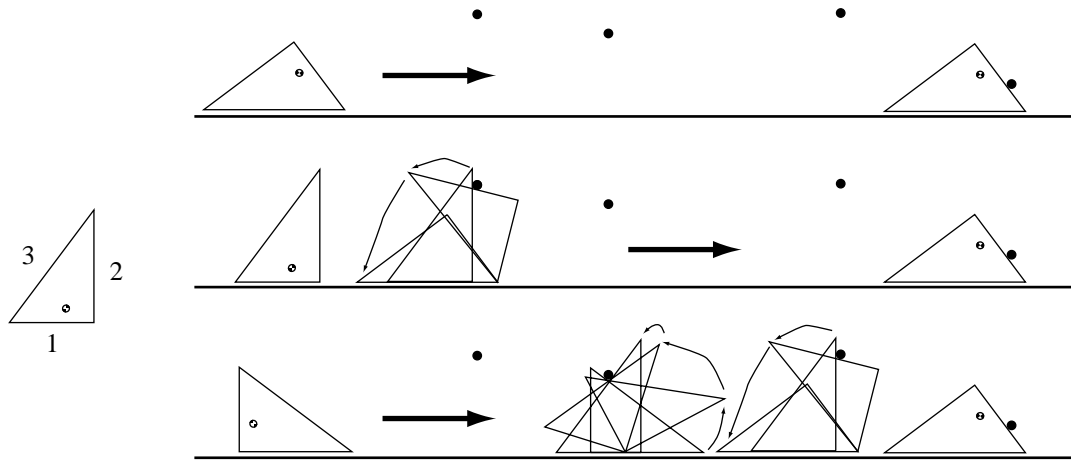


Figure 6: A sequence of fixed-height pegs that eliminates uncertainty in the part's toppling-plane orientation. At each peg, the part either passes underneath it or topples to a new edge.

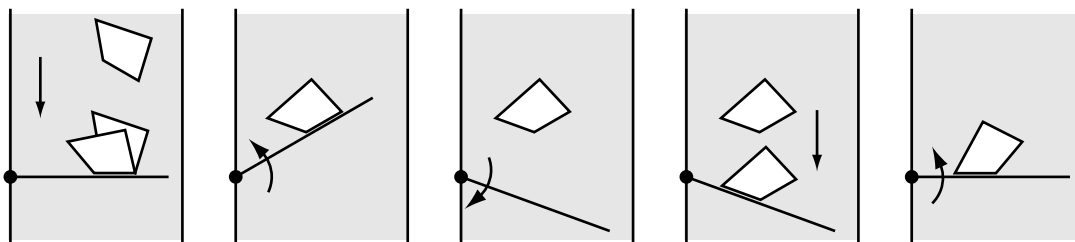


Figure 7: The 1JOC positions and orient parts in the conveyor plane by pushing.

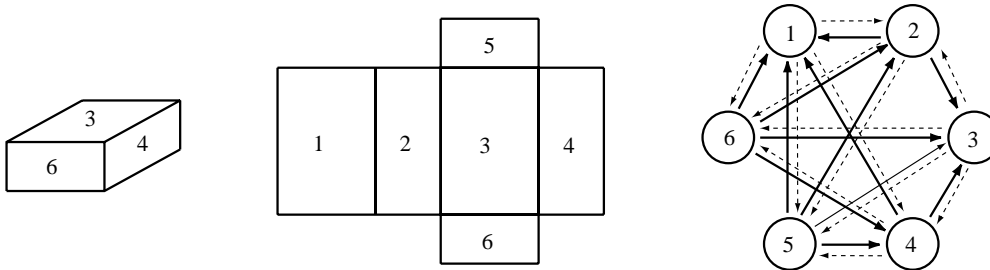


Figure 8: The toppling transition directed graph for a 3x2x1 uniform mass rectangular prism where $\mu_f = 0$ and $0.333 < \mu_c \leq 1.0$. Each node corresponds to a support face. The solid arrows correspond to transitions with feasible toppling contacts; the dotted transitions are unachievable. For $\mu_c > 1.5$, all transitions are possible.

$y > 3.881$, the peg loses contact with the triangle before it has finished rolling.) A peg at $2.361 < y < 2.698$ causes the triangle to topple from edge 2 to edge 1. No peg location will cause toppling from edge 3 to edge 2. Combining these constraints, we find that three fixed-height pegs are necessary and sufficient to bring this triangle to a unique resting edge at the end of the sequence.

In general, fixed-height fences cannot remove all toppling-plane uncertainty. These fences are analogous to the overhangs used to topple parts in bowl feeders.

3.2 2JOC

The 1JOC (1 Joint Over Conveyor) [3] performs parts feeding in the conveyor plane by using a single revolute robot joint to push parts on the conveyor (Figure 7). By combining part motion on the conveyor with a series of pushing motions, we have shown that it is possible for the 1JOC to take any polygonal part from any configuration on the conveyor (upstream of the robot) to a single desired configuration in the conveyor plane. We have also demonstrated a sensorless variant of the 1JOC.

We have augmented the 1JOC with a prismatic joint that allows the fence to move vertically, as in Figure 1. We call this system the 2JOC. The goal is to combine toppling with the ability of the 1JOC to perform conveyor-plane feeding, resulting in full 3D parts feeding on a conveyor.

For example, consider the 3x2x1 uniform mass rectangular block of Figure 8. Set $\mu_f = 0$ and $\mu_c = 0.5$. With these values, the toppling transition directed graph is shown. The part can be toppled from face A to face B when the edge AB (adjacent to faces A and B) is perpendicular to the motion of the conveyor and furthest upstream on the conveyor. Then the spatial toppling problem reduces to the planar problem above, with edge AB acting as the pivot vertex. During toppling, the fence uses its vertical prismatic motion to maintain a constant contact point on the part, but does not rotate in the conveyor plane. By sequencing 1JOC pushing and toppling, we can control the 3D configuration of the part.

If $\mu_f = 0, \mu_c > 1.5$ for the block of Figure 8, then any topple is possible; any face is reachable from any other face by toppling. In fact, for any rectangular prism with $\mu_f = 0$, there exists a μ_c^{crit} such that this property holds for all $\mu_c > \mu_c^{crit}$. This property, coupled with the 1JOC feeding property,



Figure 9: The experimental 2JOC.

indicates that any rectangular prism can be taken from any initial 3D configuration on the conveyor to a desired goal configuration, provided μ_c is sufficiently high.

Although the analysis in this paper is sufficient to analyze the 2JOC manipulating rectangular prisms, a number of issues remain for more general 3D parts. Determining which face a part will settle on is one major issue. Another is determining the full 3D force-balance conditions for rolling; in some cases, the part may undergo conveyor-plane rotation during the rolling phase of toppling. Another mechanics issue is studying the effect of out-of-plane forces in pushing (Mason and Salisbury [12]; Mayeda and Wakatsuki [13]), which are not considered in the 1JOC. We must also address automatic planning, and the existence of feasible plans as a function of the part geometry, center of mass, and μ_c and μ_f .

We have recently finished construction of a 2JOC under computer control (Figure 9), and we have implemented some simple 2JOC plans on rectangular prisms (see [1] for a description and video). Current work is toward automatic planning and execution given a general 3D part description, a goal state, and initial conditions from sensory data.

3.3 Feeding Efficiency

The Adept Flex Feeder uses a system of conveyor belts to present parts in randomized orientations to an overhead vision system. If a part in the visual field is in a graspable configuration, i.e., it is resting on the desired face, then a SCARA robot grasps the part and places it in a pallet. The conveyor remains motionless until all graspable parts in the visual field have been processed. It then advances, bringing new parts into the visual field.

When the robot moves to grasp a part, it could “bump” other parts on the way, causing them to topple onto the desired face (Goldberg [8]). The part could then be processed in the next step. This makes dual use of the robot’s motion (processing a part and preparing to process a part) which could improve the overall throughput of the system. The idea of knocking a part over to put it into a graspable configuration is similar to letting gravity reorient a part in a pivot grasp (Brock [5]; Rao *et al.* [15]).

4 Conclusions

Toppling is a mechanically simple manipulation primitive that can increase the dexterity of a simple minimalist robot. In this paper we have used a quasistatic analysis to reduce the toppling conditions to geometric contact conditions for a fixed-height fence or a one degree-of-freedom position-controlled robot operating above a conveyor. We have shown that toppling can be used in conjunction with pushing to allow a two joint robot to manipulate 3D parts on a conveyor. Remaining work includes deriving toppling transition directed graphs for 3D parts using impact simulation for the settling phase, and automatic motion planning and implementation on the 2JOC for 3D parts which are not rectangular prisms.

Acknowledgments

Thanks to Ken Goldberg for suggesting the toppling problem, Tao (Mike) Zhang for a careful reading of the paper, and Tom Scharfeld for building the 2JOC.

References

- [1] <http://lims.mech.nwu.edu/~lynch/research/2JOC/>
- [2] Y. Aiyama, M. Inaba, and H. Inoue. Pivoting: A new method of graspless manipulation of object by robot fingers. In *IEEE/RSJ International Conference on Intelligent Robots and Systems*, pages 136–143, Yokohama, Japan, 1993.
- [3] S. Akella, W. Huang, K. M. Lynch, and M. T. Mason. Parts feeding on a conveyor with a one joint robot. *Algorithmica*, to appear.
- [4] A. Bicchi and R. Sorrentino. Dexterous manipulation through rolling. In *IEEE International Conference on Robotics and Automation*, pages 452–457, 1995.
- [5] D. L. Brock. Enhancing the dexterity of a robot hand using controlled slip. In *IEEE International Conference on Robotics and Automation*, pages 249–251, 1988.
- [6] M. Brokowski, M. Peshkin, and K. Goldberg. Curved fences for part alignment. In *IEEE International Conference on Robotics and Automation*, pages 3:467–473, Atlanta, GA, 1993.
- [7] M. A. Erdmann. An exploration of nonprehensile two-palm manipulation. *International Journal of Robotics Research*, 17(5):485–503, May 1998.
- [8] K. Y. Goldberg. Personal communication, 1998.
- [9] K. M. Lynch and M. T. Mason. Dynamic nonprehensile manipulation: Controllability, planning, and experiments, 1998. *International Journal of Robotics Research*, to appear.
- [10] A. Marigo, Y. Chitour, and A. Bicchi. Manipulation of polyhedral parts by rolling. In *IEEE International Conference on Robotics and Automation*, pages 2992–2997, 1997.
- [11] M. T. Mason. Two graphical methods for planar contact problems. In *IEEE/RSJ International Conference on Intelligent Robots and Systems*, pages 443–448, Osaka, Japan, Nov. 1991.
- [12] M. T. Mason and J. K. Salisbury, Jr. *Robot Hands and the Mechanics of Manipulation*. The MIT Press, 1985.
- [13] H. Mayeda and Y. Wakatsuki. Strategies for pushing a 3D block along a wall. In *IEEE/RSJ International Conference on Intelligent Robots and Systems*, pages 461–466, Osaka, Japan, 1991.
- [14] M. A. Peshkin and A. C. Sanderson. Planning robotic manipulation strategies for workpieces that slide. *IEEE Journal of Robotics and Automation*, 4(5):524–531, Oct. 1988.
- [15] A. Rao, D. Kriegman, and K. Y. Goldberg. Complete algorithms for feeding polyhedral parts using pivot grasps. *IEEE Transactions on Robotics and Automation*, 12(6), Apr. 1996.
- [16] N. Sawasaki, M. Inaba, and H. Inoue. Tumbling objects using a multi-fingered robot. In *Proceedings of the 20th International Symposium on Industrial Robots and Robot Exhibition*, pages 609–616, Tokyo, Japan, 1989.
- [17] N. C. Singer and W. P. Seering. Utilizing dynamic stability to orient parts. *Journal of Applied Mechanics*, 54:961–966, Dec. 1987.
- [18] J. C. Trinkle and R. P. Paul. Planning for dexterous manipulation with sliding contacts. *International Journal of Robotics Research*, 9(3):24–48, June 1990.
- [19] J. C. Trinkle, R. C. Ram, A. O. Farahat, and P. F. Stiller. Dexterous manipulation planning and execution of an enveloped slippery workpiece. In *IEEE International Conference on Robotics and Automation*, pages 2: 442–448, 1993.
- [20] J. Wiegley, K. Goldberg, M. Peshkin, and M. Brokowski. A complete algorithm for designing passive fences to orient parts. In *IEEE International Conference on Robotics and Automation*, pages 1133–1139, 1996.
- [21] R. Zhang and K. Gupta. Automatic orienting of polyhedra through step devices. In *IEEE International Conference on Robotics and Automation*, pages 550–556, 1998.